Atmos. Chem. Phys. Discuss., doi:10.5194/acp-2016-1081, 2016
Manuscript under review for journal Atmos. Chem. Phys.
Published: 21 December 2016

Atmospheric Chemistry and Physics Discussions

Mixing state of oxalic acid containing particles in the rural area of Pearl River Delta, China: implication for seasonal formation mechanism of Secondary Organic Aerosol (SOA)

Chunlei Cheng[1,2], Mei Li[1,2*], Chak K. Chan[3], Haijie Tong[4], Changhong Chen[5], Duohong Chen[6], Dui Wu[1,2], Lei Li[1,2], Peng Cheng[1,2], Wei Gao[1,2], Zhengxu Huang[1,2], Xue Li[1,2], Zhong Fu[7], Yanru Bi[7], Zhen Zhou[1,2*]

[1]Institute of Mass Spectrometer and Atmospheric Environment, Jinan University, Guangzhou 510632, China
[2]Guangdong Provincial Engineering Research Center for on-line source apportionment system of air pollution, Guangzhou 510632, China
[3]School of Energy and Environment, City University of Hong Kong, Hong Kong, China
[4]Max Planck Institute for Chemistry, Multiphase Chemistry Department, Hahn-Meitner-Weg 1, 55128 Mainz, Germany
[5]State of Environmental Protection Key Laboratory of the formation and prevention of urban air pollution complex, Shanghai Academy of Environmental Sciences, Shanghai 200233, China
[6] State Environmental Protection Key Laboratory of Regional Air Quality Monitoring, Guangdong Environmental Monitoring Center, Guangzhou, 510308, China
[7]Guangzhou Hexin Analytical Instrument Limited Company, Guangzhou 510530, China

Correspondence to: Mei Li (limei2007@163.com) and Zhen Zhou (zhouzhen@gig.ac.cn)
Tel: 86-20-85225991, Fax: 86-20-85225991

Atmos. Chem. Phys. Discuss., doi:10.5194/acp-2016-1081, 2016
Manuscript under review for journal Atmos. Chem. Phys.
Published: 21 December 2016

Atmospheric Chemistry and Physics Discussions

Abstract:

The formation of oxalic acid and its mixing state in atmospheric particulate matter (PM) were studied using a single particle aerosol mass spectrometer (SPAMS) in the summer and winter of 2014 in Heshan, a supersite in the rural area of the Pearl River Delta (PRD) region in China. Oxalic acid-containing particles accounted for 2.5% and 2.7% in total detected ambient particles in summer and winter, respectively. Oxalic acid was measured in particles classified as elemental carbon (EC), organic carbon (OC), elemental and organic carbon (ECOC), biomass burning (BB), heavy metal (HM), secondary (Sec), sodium-potassium (NaK) and dust. Oxalic acid was found predominantly mixing with sulfate and nitrate during the whole sampling period, likely due to aqueous phase reactions. In summer, oxalic acid-containing particle number and ozone concentration followed a very similar trend, which may reflect the significant contribution of photochemical reactions to oxalic acid formation. Furthermore, favorable in-situ pH (2-4) conditions were observed, which promote Fenton like reactions for efficient production of •OH in HM type particles. A mechanism in which products of photochemical oxidation of VOCs partitioned into the aqueous phase of HM particles, followed by multistep oxidation of •OH through Fenton like reactions to form oxalic acid is proposed. In wintertime, carbonaceous type particles contained a substantial amount of oxalic acid as well as abundant carbon clusters and biomass burning markers. The general existence of nitric acid in oxalic acid-containing particles indicates an acidic environment during the formation process of oxalic acid. Organosulfate-containing particles well correlated with oxalic acid-containing particles during the episode, which suggests the formation of oxalic acid is closely associated with acid-catalyzed reactions of organic precursors.

Keywords: Oxalic acid; Single particles; Mixing state; Photochemical process; Secondary organic aerosols.

Atmos. Chem. Phys. Discuss., doi:10.5194/acp-2016-1081, 2016
Manuscript under review for journal Atmos. Chem. Phys.
Published: 21 December 2016

Atmospheric Chemistry and Physics Discussions

1. Introduction

Organic aerosol, typically a large fraction of fine particles, contains more than thousands of organic compounds and contributes to visibility reduction, photochemical smog, climate change and adverse health effects (Novakov and Penner, 1993;Goldstein and Galbally, 2007;Jimenez et al., 2009;Poschl and Shiraiwa, 2015). A significant component of organic aerosol is secondary organic aerosol (SOA) formed from the gas phase oxidation of volatile organic compounds (VOCs) followed by partitioning of products into particles or from heterogeneous reactions of VOCs with particles (Hallquist et al., 2009;Zhang et al., 2015). Dicarboxylic acids (DCAs) are abundant and ubiquitous constituents in SOA and can be effective tracers for the oxidative processes leading to the formation of SOA (Kawamura and Ikushima, 1993;Ervens et al., 2011;Wang et al., 2012;Cheng et al., 2013). DCAs normally have high water solubility and low vapor pressure, so they play important roles in controlling the hygroscopic properties of organic aerosols (Prenni et al., 2003;Ma et al., 2013) and activating cloud condensation nuclei (Booth et al., 2009). The primary emissions of DCAs from anthropogenic sources are minor (Huang and Yu, 2007;Stone et al., 2010), and they are mainly derived from secondary oxidation of VOCs and subsequent intermediates (Ho et al., 2010;Myriokefalitakis et al., 2011). Even though high concentrations of DCAs have been observed in air masses influenced by biomass burning (Kundu et al., 2010;Kawamura et al., 2013), the primary source of DCAs is still not clear (van Pinxteren et al., 2014).

The production of DCAs through photochemical reactions has been reported in many field studies via the analysis of the diurnal and seasonal variations of DCA(Kawamura and Ikushima, 1993;Kawamura and Yasui, 2005;Aggarwal and Kawamura, 2008;Pavuluri et al., 2010;Ho et al., 2011), but the mechanism of DCAs formation is still not well understood. Oxalic acid is usually the most abundant DCA observed in the field (Kawamura et al., 2004;Ho et al., 2007;Kawamura et al., 2010). Several studies have found a tight correlation between oxalic acid and sulfate in ambient particles, implying that aqueous chemistry leads to the formation of oxalic

Atmos. Chem. Phys. Discuss., doi:10.5194/acp-2016-1081, 2016
Manuscript under review for journal Atmos. Chem. Phys.
Published: 21 December 2016

acid in aerosols and cloud droplets (Yao et al., 2002;Yao et al., 2003;Yu et al., 2005;Sorooshian et al., 2007;Miyazaki et al., 2009). In recent years, many model and laboratory studies suggest that the aqueous phase oxidation of highly water-soluble organics like glyoxal, methylglyoxal and glyoxylic acid can efficiently produce oxalic acid in aerosol particles and cloud droplets (Lim et al., 2010;Myriokefalitakis et al., 2011;Ervens et al., 2014;Yu et al., 2014;McNeill, 2015). Recent stable carbon isotope studies and field observations have also suggested that oxalic acid forms through aqueous phase reactions (Wang et al., 2012;Cheng et al., 2015). However, the exact formation pathways of oxalic acid in ambient particles are still unknown due to the complexity of meteorological condition and the temporal resolution limitations of conventional filter sampling studies and bulk chemical analysis.

Online measurements of the size distribution of oxalic acid-containing particles and the mixing state of oxalic acid with other compounds in aerosols are useful to examine the formation and evolution of oxalic acid and SOA particles. Sullivan and Prather investigated the diurnal cycle and mixing state of DCA-containing particles in Asian aerosol outflow using aerosol time-of-flight mass spectrometry (ATOFMS), and proposed the formation of DCA on Asian dust (Sullivan and Prather, 2007). In addition, Yang et al. (2009) measured oxalic acid particles in Shanghai and proposed that in-cloud processes and heterogeneous reactions on hydrated aerosols contributed to the formation of oxalic acid (Yang et al., 2009). So far the formation mechanism of oxalic acid especially in urban areas is still not clear. Online measurements of the mixing state of oxalic acid provides a powerful context to better understand the formation of oxalic acid in aerosol particles and cloud droplets.

The Pearl River Delta (PRD) region has distinct meteorological seasonality under the influence of the Asian monsoon system, which brings air from the ocean in spring and summer, and carries polluted air from northern China in autumn and winter. Strong photochemical activity occurs in summer under the condition of high temperature and relative humidity, and in winter high loadings of particles from northern cities are favorable for the occurrence of haze episode (Bi et al., 2011;Zhang et al., 2013;Zhang et al., 2014). Here we present the seasonal field measurements of

Atmos. Chem. Phys. Discuss., doi:10.5194/acp-2016-1081, 2016
Manuscript under review for journal Atmos. Chem. Phys.
Published: 21 December 2016

the mixing state of oxalic acid-containing particles using a single particle aerosol mass spectrometer (SPAMS) in a rural supersite of the PRD region. The seasonal characteristic of oxalic acid particles and mixing state with secondary species were investigated to explore the formation mechanisms of oxalic acid and aging process of SOA.

2. Methods

2.1 Aerosol sampling

Particles were sampled using a single particle aerosol mass spectrometer (SPAMS) at the Guangdong Atmospheric Supersite (22.73N, 112.93E), a rural site at Heshan city (Figure S1). The supersite is surrounded by farm land and villages, with no local industrial or traffic emissions. Ambient aerosols were sampled to the SPAMS through a 2.5m long copper tube with 0.5m of the sampling inlet located above the top of the building. The measurement period was from July 18 to August 1 in 2014, and from January 27 to February 8 in 2015. Real-time $PM_{2.5}$ mass concentration was simultaneously measured by a TEOM monitor (series 1405, Thermo scientific), and hourly concentrations of O_3 were measured by an O_3 analyzer (model 49i, Thermo scientific). The local meteorological data including temperature, relative humidity and visibility were measured on the rooftop of the building. The average temperature during the field study was 29.5 ℃ in summer and 14.1 ℃ in winter and the average relative humidity was 71.7% and 63% in summer and winter, respectively.

2.2 SPAMS

Real-time measurements of single atmospheric particles has been demonstrated by Prather and co-workers in the 1990s using aerosol time-of-flight mass spectrometry (ATOFMS) (Prather et al., 1994;Noble and Prather, 1996). Based on the same principle, the single particle aerosol mass spectrometer (SPAMS) developed by Guangzhou Hexin Analytical Company was applied to field measurements of single particles in the current work. The details of the SPAMS system have been introduced previously (Li et al., 2011). Briefly, aerosol particles are sampled into the vacuum pumped aerodynamic lens of the SPAMS through an electro-spark machined 80μm

Atmos. Chem. Phys. Discuss., doi:10.5194/acp-2016-1081, 2016
Manuscript under review for journal Atmos. Chem. Phys.
Published: 21 December 2016

Atmospheric Chemistry and Physics Discussions

critical orifice at a flow rate of 75 ml min^{-1}. The individual particles with a terminal velocity are introduced to the sizing region. The velocity of each single particle is detected by two continuous laser beams (diode Nd:YAG, 532 nm) with a space of 6 cm. The velocity is then used to calculate the single particle aerodynamic diameter and provide the precise timing of the firing of a 266 nm laser used to induce desorption and ionization (Nd:YAG laser, 266nm). The energy of the desorption/ionization 266 nm laser was 0.6 mJ and the power density was kept at about 1.6×10^{8} W/cm^{2} during both sampling periods. The 266 nm laser generates positive and negative ions that are detected by a Z-shaped bipolar time of flight mass spectrometer. The size range of the detected single particles is 0.2 to 2 μm. Polystyrene latex spheres (Nanosphere size standards, Duke Scientific Corp., Palo Alto) of 0.22-2.0 μm diameter were used for size calibration.

2.3 Data analysis

The size and chemical composition of single particles detected by SPAMS were analyzed using the COCO toolkit based on the Matlab software. Particles were clustered into several groups using the neural network algorithm (ART-2a) to group particles into clusters with similar mass spectrum features. The ART-2a parameters used in this work were set to a vigilance factor of 0.8, a learning rate of 0.05, and a maximum of 20 iterations. We collected 516,679 and 767,986 particles with both positive and negative mass spectra in summer and winter respectively. A standard solution of oxalic acid was prepared with pure oxalic acid ($H_2C_2O_4$, purity: 99.99%, Aladdin Industrial Corporation) and atomized to aerosols. After drying through two silica gel diffusion driers, pure oxalic acid particles were directly introducing into the SPAMS. The positive and negative mass spectra of oxalic acid are shown in Figure S2. Based on the mass spectra of pure oxalic acid and previous ambient measurements by ATOFMS (Silva and Prather, 2000;Sullivan and Prather, 2007;Yang et al., 2009), $HC_2O_4^-$ (m/z -89) is selected as the ion peak for oxalic acid containing particles. In this work, oxalic acid particles are identified if the peak area of m/z -89 was larger than 0.5% of the total signal in the mass spectrum. With this threshold, 13109 and 20504 of oxalic acid-containing particles were obtained in summer and winter

Atmos. Chem. Phys. Discuss., doi:10.5194/acp-2016-1081, 2016
Manuscript under review for journal Atmos. Chem. Phys.
Published: 21 December 2016

separately, accounting for 2.5% and 2.7% of the total detected particles. According to characteristic ion markers and dominant chemical species (Table S1), all oxalic acid particles were classified into eight types: elemental carbon (EC), organic carbon (OC), elemental and organic carbon (ECOC), biomass burning (BB), heavy metal (HM), secondary (Sec), sodium-potassium (NaK) and dust.

2.4 Inorganic ions and in-situ pH (pH_{is})

Water-soluble inorganic ions and trace gases were determined by an online analyzer for monitoring aerosols and gases (MARGA, model ADI 2080, Applikon Analytical B. V. Corp., the Netherlands) with a $PM_{2.5}$ sampling inlet at one hour resolution from July 18 to August 1 in 2014. The principle and instrumental design has been described in detail elsewhere (ten Brink et al., 2007;Du et al., 2011;Behera et al., 2013;Khezri et al., 2013). Standard solutions containing all detected ions were injected into MARGA before and after the field measurement. The liquid water content and the concentration of H^+ in particles are calculated using the ISORROPIA II model (Nenes et al., 1998, 1999;Fountoukis and Nenes, 2007). The in-situ pH (pH_{is}) of particles is calculated through the following equation:

$$pH_{is} = -\log\alpha_{H^+} = -\log(\gamma_{H^+} \times n_{H^+} \times 1000/V_a) \quad (1)$$

where n_{H^+} is the concentration of H^+ (mol m^{-3}) and V_a is the volume concentration of the H_2O (cm^3 m^{-3}) , while γ_{H^+} is the activity coefficient of H^+(Xue et al., 2011;Cheng et al., 2015). The temporal variation of pH_{is} of ambient $PM_{2.5}$ particles is presented in Figure S3, and demonstrated that 97% of particles were acidic in summer.

3. Results and Discussion

3.1 Seasonal variation of oxalic acid containing particles

The clustered 48 hr back trajectories of air masses arriving in Heshan during the sampling period are shown in Figure S4. In summer, air masses at 500m levels above the ground were mainly from the ocean and rural areas with less influence of human activity, while in winter air masses were directly from urban areas of Guangzhou and Foshan, indicating a strong influence from anthropogenic emissions. The temporal

Atmos. Chem. Phys. Discuss., doi:10.5194/acp-2016-1081, 2016
Manuscript under review for journal Atmos. Chem. Phys.
Published: 21 December 2016

variations of the total detected particles and oxalic acid containing particles in summer and winter are shown in Figure 1. The total particles had similar trends with the mass concentration of ambient $PM_{2.5}$, suggesting that the counts of total particles detected by SPAMS can be representative of $PM_{2.5}$ mass concentration during the whole sampling periods. The oxalic acid (C_2-containing) particles, in general, exhibited distinct diurnal peaks from July 28 to August 1, while they showed different temporal trends in winter. The relative abundance of oxalic acid particles in all of the sampled particles (C_2/total ratio) had the same variations with the abundance of oxalic acid particles in summer, especially in the period of July 28 – August 1 (Figure 1). In winter, however, particle counts and relative abundance of oxalic acid had different temporal changes except Jan 30 and February 5-8, when the count and relative abundance of oxalic acid particles simultaneously had a sudden increase.

The oxalic acid-containing particles were clustered into eight groups, and they altogether accounted for 89.6% and 95.1% of total oxalic acid particles in summer and winter, respectively. Table 1 shows that in summer heavy metal (HM) type particles contributed 31.3% to total oxalic acid particles, followed by the Sec (19.2%) and BB type (13%). However, in winter BB type particles were the most abundant and accounted for 24.2% of the oxalic acid-containing particles, followed by EC and HM type. Besides, carbonaceous type particles including EC, OC, ECOC and BB accounted for 28.1% of oxalic acid particles in summer and 59.8% in winter, indicating the seasonal different characteristics of oxalic acid particles. The temporal variations of eight groups of oxalic acid particles in summer and winter are illustrated in Figure 1. In summer HM type particles (purple) and total oxalic acid particles exhibited similar diurnal patterns, suggesting a possibly connection between the production of oxalic acid and the transition metals (e.g. Fe, Cu) (Sorooshian et al., 2013). Although Sec, BB and EC type particles showed similar diurnal patterns with total oxalic acid particles, the concentrations of these type particles were generally lower than HM type particles. In winter diurnal variation of oxalic acid particles was not obvious but a sharp increase, accompanied by the increase of BB, EC and Sec type particles, was observed on February 8.

Atmos. Chem. Phys. Discuss., doi:10.5194/acp-2016-1081, 2016
Manuscript under review for journal Atmos. Chem. Phys.
Published: 21 December 2016

Atmospheric Chemistry and Physics Discussions

The averaged positive and negative ion mass spectra of oxalic acid containing particles are shown in Figure 2. The positive ion spectrum of oxalic acid particles in summer was characterized by high fractions of metal ion peaks including 23$[Na]^+$, 27$[Al]^+$, 39$[K]^+$, 55$[Mn]^+$, 56$[Fe]^+$, 63/65$[Cu]^+$,64$[Zn]^+$ and 208$[Pb]^+$, and carbonaceous marker ions at m/z 27$[C_2H_3]^+$, 36$[C_3]^+$, 43$[C_2H_3O/C3H7]^+$, 48$[C_4]^+$ (Figure 2 a). The negative ion spectrum of oxalic acid particles in summer was characterized by the strong intensity of secondary ions including m/z -46$[NO_2]^-$, -62$[NO_3]^-$, -79$[PO_3]^-$, -80$[SO_3]^-$, -96$[SO_4]^-$ and -97$[HSO_4]^-$, as well as carbon clusters of -24$[C_2]^-$, -36$[C_3]^-$, -48$[C_4]^-$ and BB markers of -59$[C_2H_3O_2]^-$ and -73$[C_3H_5O_2]^-$ (Figure 2 b) (Zauscher et al., 2013). More carbonaceous clusters, i.e., 27$[C_2H_3]^+$, 29$[C_2H_5]^+$, 36$[C_3]^+$, 37$[C_3H]^+$, 43$[C_2H_3O]^+$, 48$[C_4]^+$, 51$[C_4H_3]^+$, 55$[C_4H_7]^+$, 60$[C_5]^+$, 63$[C_5H_3]^+$, 65$[C_5H_5]^+$, 74$[C_2H_2O_3]^+$, 77$[C_6H_5]^+$, were observed in the positive ion spectrum of oxalic acid particles in winter (Figure 2 c) than in summer. The negative ion spectrum of oxalic acid particles in winter (Figure 2 d) contained a large amount of secondary ions, similar to those found in summer, and a more intense signal of nitric acid (-125$[HNO_3NO_3]^-$) , suggesting an acidic nature of oxalic acid particles in winter.

The mixing ratios of oxalic acid particles with sulfate, nitrate and ammonium (SNA) were investigated through the relative abundance of SNA-containing oxalic acid particles in total oxalic acid particles (Figure 3). Oxalic acid was found to be internally mixed with sulfate and nitrate during both sampling periods with mixing ratio of 93% and 94% in summer respectively, and both 98% in winter (Figure 3 a). However, the mixing ratio of NH_4^+ with oxalic acid was only 18% in summer but increased to 71% in winter. Linear correlations between NH_4^+-containing oxalic acid particles (C_2-NH_4^+) and total oxalic acid particles are depicted in Figure 3, with better linear regression (r^2=0.98) in winter than summer. The low mixing ratio of NH_4^+ in oxalic acid particles in summer indicated that the presence of oxalic acid in NH_4^+-poor particles. Aqueous phase production of SO_4^{2-} has been studied well and the linear correlation between oxalic acid and SO_4^{2-} has been used to study the production of oxalic acid through aqueous phase reactions (Yu et al., 2005;Miyazaki et al.,

Atmos. Chem. Phys. Discuss., doi:10.5194/acp-2016-1081, 2016
Manuscript under review for journal Atmos. Chem. Phys.
Published: 21 December 2016

Atmospheric Chemistry and Physics Discussions

2009;Cheng et al., 2015). In our work, oxalic acid and C_2-SO_4^{2-} displayed good correlations in summer and winter (both r^2=0.99), which suggests a common production route of oxalic acid and sulfate, likely aqueous phase reactions.

Figure 4 shows the unscaled size-resolved number distributions of the eight types of oxalic acid particles. Oxalic acid mainly existed in 0.4 to 1.2 μm particles during the entire sampling period but exhibited different peak modes for each particle type in summer and winter. In summer, major types of oxalic acid particles showed distinct peak mode at different size diameter. EC and Sec type particles peaked at 0.5 μm, followed by BB type particles at 0.55 μm, then HM type particles at 0.6 μm, and OC type particles at 0.7 μm. The difference of peak mode suggests possibly different chemical evolution process for each type oxalic acid-containing particles. However, in winter, oxalic acid particles showed broader size distribution from 0.5 to 0.8 μm for all particle types. Oxalic acid particles of all types were generally larger in winter than summer, possibly due to condensation and coagulation of particles during aging of oxalic acid particles in winter.

3.2 Photochemical production of oxalic acid in summer

In summer oxalic acid particles showed peaks in the afternoon especially from July 28 to August 1, which was in agreement with the variation pattern of the O_3 concentration (Figure 5), indicating a strong association of oxalic acid formation with photochemical reactions. Malonic acid is another product of photochemical oxidation of organic compounds (Kawamura and Ikushima, 1993;Wang et al., 2012;Meng et al., 2013;Meng et al., 2014). In our campaign, malonic acid containing particles had diurnal trends similar to oxalic acid particles and O_3 concentration. As the dominant particle type, HM particles had identical variation pattern with total oxalic acid particles. They are characterized by highly abundant metal ion peaks like 55$[Mn]^+$, 56$[Fe]^+$, 63/65$[Cu]^+$, 64$[Zn]^+$ and 208$[Pb]^+$, as well as secondary ion peaks of -46$[NO_2]^-$, -62$[NO_3]^-$, -80$[SO_3]^-$, -96$[SO_4]^-$ and -97$[HSO_4]^-$ in the negative spectrum in summer (Figure 6). •OH produced from Fenton reactions between H_2O_2 and $Fe^{2+/3+}$ in acidic solutions has been considered as a substantial source of •OH(Fenton, 1894;Dunford, 2002;Herrmann et al., 2015). The high abundance of metal ions in

Atmos. Chem. Phys. Discuss., doi:10.5194/acp-2016-1081, 2016
Manuscript under review for journal Atmos. Chem. Phys.
Published: 21 December 2016

oxalic acid particles may be an indication of possible Fenton reactions in the acidic aqueous phase of acidic particles (pH<5, Figure S3), although we cannot exclude the possibility of gas phase condensation of oxalic and malonic acids onto HM particles.

The oxidation of glyoxal and glyoxylic acid by •OH has been identified as an important pathway of oxalic acid production by field and laboratory studies (Ervens et al., 2004;Ervens and Volkamer, 2010;Wang et al., 2012). The modeling studies from Ervens et al. (2014) suggest that oxalic acid production from glyoxal and glyoxylic acid in aqueous phase significantly depends on •OH availability (Ervens et al., 2014). While the partition of •OH from gas to aqueous phase is limited by its low Henry's law constant ($K_{H,OH}$=30 M atm^{-1}) and short lifetime of •OH in the gas phase (Hanson et al., 1992), the main sources of aqueous •OH are from the photolysis of H_2O_2, NO_3^-, NO_2^-, and chromophoric dissolved organic matter (CDOM) (Yu et al., 2014;Badali et al., 2015;Gligorovski et al., 2015;Tong et al., 2016). Among these sources the photolysis of H_2O_2 through Fenton reactions involving the catalysis of transition metal ions like $Fe^{2+/3+}$, $Cu^{+/2+}$ and $Mn^{2+/3+}$ is an efficient source of •OH (Deguillaume et al., 2005;Herrmann et al., 2005;Ervens et al., 2014). The •OH formation process through Fenton reactions can be expressed as (Ervens, 2015):

$$Fe^{2+} + H_2O_2 \rightarrow FeOH^{2+} + \bullet OH \quad (\text{or } Fe^{3+} + OH^- + \bullet OH) \qquad (R1)$$

$$FeOH^{2+}/Fe^{3+} + HO_2^{\cdot}/O_2^{\cdot-} \rightarrow Fe^{2+} + O_2 + H_2O/OH^- \qquad (R2)$$

The actual chemical process is far more complex and involves iron oxides and iron-complexes, thus in the current work we focus on the potential availability of •OH from Fenton reactions and the impact on the oxidation process of organic precursors.

In order to investigate the photochemical aqueous phase formation of oxalic acid in summer, the diurnal variations of O_3, oxalic acid particles, HM group particles and pH_{is} of ambient particles averaged from July 28 to August 1, 2014 are shown in Figure 7. The concentration of O_3 increased after 9:00 and peaked at 17:00, while oxalic acid particles and HM group particles both increased after 10:00 and showed two peaks at 15:00 and 19:00. The prominent photochemical feature of oxalic acid particles suggested a close association of photochemical reactions with oxalic acid production. Although •OH production from Fenton reactions can both occur under

Atmos. Chem. Phys. Discuss., doi:10.5194/acp-2016-1081, 2016
Manuscript under review for journal Atmos. Chem. Phys.
Published: 21 December 2016

Atmospheric Chemistry and Physics Discussions

dark and light radiation conditions, only photo-Fenton reactions had significant contribution to the enhancement of oxalic acid particles in the current work. This was possibly due to the diurnal variation of pH_{is}, since Fenton reactions strongly depend on the pH of the aqueous phase (Gligorovski et al., 2015). When pH<1, Fe^{2+} is directly oxidized by H_2O_2 to Fe^{3+} with no production of •OH (Barb et al., 1951;Kremer, 2003), and the most favorable pH value for Fenton reaction is between 2.5 and 5 (Deguillaume et al., 2005). In the current work the pH_{is} of ambient particles ranged from -1.42 to 4.01, and the influences of pH_{is} from RH and inorganic ions are discussed in Figure S5. Strongly acidic particles were observed during the whole day with high pH_{is} at 6:00 and after 12:00. Although pH_{is} was around 2 at 6:00, only a few oxalic acid-containing particles were observed during this period due to low abundance of HM particles. Oxalic acid-containing particles were found to increase from 12:00 to 21:00, which was attributed to increased organic precursors from VOCs oxidation and enhanced •OH production from Fenton reactions under pH_{is} at 1-4. The number concentration of oxalic acid particles peaked at 19:00 instead of during the strong photochemical activity period in the afternoon; this was possibly due to the efficient degradation of oxalic acid from the complex of $Fe(oxalate)_2^-$ (Sorooshian et al., 2013;Zhou et al., 2015). On the other hand, photolysis of $Fe(oxalate)_2^-$ can contribute to 99% of the overall degradation of oxalic acid (Weller et al., 2014). Although the enhanced •OH production from photo-Fenton reactions was favorable for the formation of oxalic acid from 12:00 to 18:00, we speculate that a high degradation rate of oxalic acid by iron complexation resulted in a lower net production of oxalic acid than at 19:00.

Based on above discussions, detailed mechanism for oxalic acid formation in acidic aqueous phase of particles is proposed for our field observations (Figure 8). In summer strong photochemical activity and high O_3 concentrations in the afternoon leads to more production of reactive radicals such as •OH and $HO_2^{\bullet}$, which promote the oxidation of VOCs to dicarbonyls and aldehydes (e.g. glyoxal and methylglyoxal), followed by a subsequent partitioning into the aqueous phase of particles (Myriokefalitakis et al., 2011). Acidic particles containing transition metals like Fe

Atmos. Chem. Phys. Discuss., doi:10.5194/acp-2016-1081, 2016
Manuscript under review for journal Atmos. Chem. Phys.
Published: 21 December 2016

Atmospheric Chemistry and Physics Discussions

and Cu potentially yield more •OH in acidic aqueous phase, then hydrated dicarbonyls and aldehydes can be oxidized by •OH to glyoxylic acid and finally to oxalic acid (Wang et al., 2012). Recently Ma et al. (2015) had studied the Fe-containing particles in the PRD and found Fe-containing particles are more efficient at generating •OH in summer than winter (Ma et al., 2015), which supports the enhanced •OH production in HM type particles in this work. A large amount of Fe related particles are emitted from steel industries in the North China Plain and metals like V, Zn, Cu and Pb from electronic manufacturing (Cui and Zhang, 2008;Dall'Osto et al., 2008). These metals contribute significantly to haze episodes (Moffet et al., 2008;Li et al., 2014), which possibly increases the formation of SOA by yielding more OH participating the heterogeneous and aqueous reactions.

3.3 Formation process of oxalic acid in winter

Despite lower O_3 concentrations and photochemical activity in winter, oxalic acid particles were still prevalent in carbonaceous particles, especially BB type particles. The sharp increase of oxalic acid particles on February 8, 2015 (Figure 1) was selected as a typical episode to investigate the formation processes of oxalic acid in winter.

During the episode, the 48 hr back trajectory analysis showed air masses that originated from the urban areas of Guangzhou and Foshan city (Figure S4), indicating strong influence on organic precursors from anthropogenic emissions. Oxalic acid particle types were dominated by BB (23.2%), followed by EC (22.0%) and Sec (15.1%) type (Table 2). Carbonaceous particles including EC, ECOC, OC, BB accounted for 61.6% of the total oxalic acid particles. The mass spectra of oxalic acid particles were characterized by many hydrocarbon clusters of 27$[C_2H_3]^+$, 29$[C_2H_5]^+$, 37$[C_3H]^+$, 43$[C_2H_3O]^+$, 51$[C_4H_3]^+$, 55$[C_4H_7]^+$, 63$[C_5H_3]^+$, 65$[C_5H_5]^+$, 74$[C_2H_2O_3]^+$, 77$[C_6H_5]^+$, and carbon clusters of 36$[C_3]^+$, 48$[C_4]^+$, 60$[C_5]^+$ in positive mass spectrum, while the negative mass spectrum was characterized by elemental carbon clusters like -24$[C_2]^-$, -36$[C_3]^-$, -48$[C_4]^-$, biomass burning markers of -59$[C_2H_3O_2]^-$ and -73$[C_3H_5O_2]^-$ and secondary species including -42$[CNO]^-$, -46$[NO_2]^-$, -62$[NO_3]^-$, -79$[PO_3]^-$, -80$[SO_3]^-$, -96$[SO_4]^-$ and -97$[HSO_4]^-$ (Figure 9 a). The nitric acid was

Atmos. Chem. Phys. Discuss., doi:10.5194/acp-2016-1081, 2016
Manuscript under review for journal Atmos. Chem. Phys.
Published: 21 December 2016

identified in oxalic acid particles not only in the episode but also during the entire sampling period in winter, indicating a strongly acidic nature of oxalic acid particles in winter.

As the precursor of oxalic acid, glyoxal has the potential to react with sulfuric acid to produce organosulfates through acid-catalyzed nucleophilic addition according to laboratory and chamber studies(Surratt et al., 2007;Galloway et al., 2009). The negative ion of -155($[C_2H_3O_2SO_4]^-$) has been identified as the marker ion of organosulfates derived from glyoxal in chamber and field measurements using ATOFMS (Surratt et al., 2008;Hatch et al., 2011). The organosulfate derived from glyoxal requires acidic aqueous environment of particles, and herein is used as an indicator of acid-catalyzed ageing process of organic compounds. The temporal variation of organosulfate (m/z=-155) containing particles during the entire sampling period in Heshan, China is shown in Figure S6. During the episode, oxalic acid particles had moderate linear correlation with organosulfate particles (Figure 9b). Based on the above discussion, the degradation of carbonaceous species associated with acid-catalyzed reactions may have a significant contribution to the formation of oxalic acid during the episode in winter. Similar particle types and mass spectra of oxalic acid-containing particles during the episode and the whole sampling period in winter were observed, which suggest the acid-catalyzed oxidation of organic precursors as a potential source for oxalic acid.

4. Summary and conclusions

Oxalic acid containing particles were measured by a single particle aerosol mass spectrometer (SPAMS) in the summer and winter of 2014 in Heshan, China. They accounted for 2.5% and 2.7% of the total detected ambient particles. In summer heavy metal-containing particles were the largest group of particles containing oxalic acid with a fraction of 31.3% followed by Sec type (19.2%), while in winter BB type was the dominant group with a percentage of 24.2%. More than 90% of oxalic acid particles were internally mixed with sulfate and nitrate during the whole sampling period. Only 18% of oxalic acid particles contained ammonium in summer, which

increased to 71% in winter. In summer oxalic acid and O_3 concentration exhibited similar diurnal variations, indicating a substantial contribution of photochemical reactions to oxalic acid formation. The favorable in-situ pH and the dominance of transition metal ions in oxalic acid particles suggests an enhanced production of •OH from Fenton like reactions. A mechanism involving the photochemical production of VOCs via efficient aqueous phase reactions with enhanced •OH to oxalic acid was proposed. In winter carbonaceous type particles including EC, OC, ECOC and BB groups accounted for 59.8% of oxalic acid particles and increased to 61.6% in the episode. Nitric acid and organosulfate were found to co-exist in oxalic acid-containing particles in the winter, which suggests a close association with acid-catalyzed reactions. Acid-catalyzed oxidation of organic precursors is a potential contribution for the formation of oxalic acid in winter. The current study also indicates that SPAMS can be a robust tool for exploring the formation and transformation processes of SOA, contributing to the improvement of global climate modeling and the development of effective air pollution mitigation strategies.

Acknowledgments

This work was financially supported by National Key Technology R&D Program (Grant No. 2014BAC21B01), Guangdong Province Public Interest Research and Capacity Building Special Fund (Grant No. 2014B020216005), the Strategic Priority Research Program (B) of the Chinese Academy of Sciences (Grant No. XDB05040502), Guangdong Industry-University Research Program (Grant No.2012B090500014), and NSFC of Guangdong Province (Grant No. 2015A030313339). Chak K. Chan would like to acknowledge funding support of the General Fund of National Natural Science Foundation of China (Grant No. 41675117).

References

Aggarwal, S. G., and Kawamura, K.: Molecular distributions and stable carbon isotopic compositions of dicarboxylic acids and related compounds in aerosols from Sapporo, Japan: Implications for photochemical aging during long-range atmospheric transport, Journal of Geophysical Research-Atmospheres, 113, D14301, 10.1029/2007jd009365, 2008.

456 Badali, K. M., Zhou, S., Aljawhary, D., Antinolo, M., Chen, W. J., Lok, A., Mungall, E., Wong, J.
457 P. S., Zhao, R., and Abbatt, J. P. D.: Formation of hydroxyl radicals from photolysis of
458 secondary organic aerosol material, Atmospheric Chemistry and Physics, 15, 7831-7840,
459 10.5194/acp-15-7831-2015, 2015.
460 Barb, W., Baxendale, J., George, P., and Hargrave, K.: Reactions of ferrous and ferric ions with
461 hydrogen peroxide. Part I.—The ferrous ion reaction, Transactions of the Faraday Society, 47,
462 462-500, 1951.
463 Behera, S. N., Betha, R., Liu, P., and Balasubramanian, R.: A study of diurnal variations of PM 2.5
464 acidity and related chemical species using a new thermodynamic equilibrium model, Science of
465 the Total Environment, 452, 286-295, 2013.
466 Bi, X., Zhang, G., Li, L., Wang, X., Li, M., Sheng, G., Fu, J., and Zhou, Z.: Mixing state of
467 biomass burning particles by single particle aerosol mass spectrometer in the urban area of PRD,
468 China, Atmospheric Environment, 45, 3447-3453, 2011.
469 Booth, A. M., Topping, D. O., McFiggans, G., and Percival, C. J.: Surface tension of mixed
470 inorganic and dicarboxylic acid aqueous solutions at 298.15 K and their importance for cloud
471 activation predictions, Phys Chem Chem Phys, 11, 8021-8028, 10.1039/b906849j, 2009.
472 Cheng, C., Wang, G., Meng, J., Wang, Q., Cao, J., Li, J., and Wang, J.: Size-resolved airborne
473 particulate oxalic and related secondary organic aerosol species in the urban atmosphere of
474 Chengdu, China, Atmospheric Research, 161, 134-142, 2015.
475 Cheng, C. L., Wang, G. H., Zhou, B. H., Meng, J. J., Li, J. J., Cao, J. J., and Xiao, S.: Comparison
476 of dicarboxylic acids and related compounds in aerosol samples collected in Xi'an, China during
477 haze and clean periods, Atmospheric Environment, 81, 443-449,
478 10.1016/j.atmosenv.2013.09.013, 2013.
479 Cui, J. R., and Zhang, L. F.: Metallurgical recovery of metals from electronic waste: A review, J
480 Hazard Mater, 158, 228-256, 10.1016/j.jhazmat.2008.02.001, 2008.
481 Dall'Osto, M., Booth, M., Smith, W., Fisher, R., and Harrison, R. M.: A study of the size
482 distributions and the chemical characterization of airborne particles in the vicinity of a large
483 integrated steelworks, Aerosol Science and Technology, 42, 981-991, 2008.
484 Deguillaume, L., Leriche, M., Desboeufs, K., Mailhot, G., George, C., and Chaumerliac, N.:
485 Transition metals in atmospheric liquid phases: Sources, reactivity, and sensitive parameters,
486 Chem Rev, 105, 3388-3431, 10.1021/cr040649c, 2005.
487 Du, H., Kong, L., Cheng, T., Chen, J., Du, J., Li, L., Xia, X., Leng, C., and Huang, G.: Insights
488 into summertime haze pollution events over Shanghai based on online water-soluble ionic
489 composition of aerosols, Atmospheric Environment, 45, 5131-5137, 2011.
490 Dunford, H. B.: Oxidations of iron (II)/(III) by hydrogen peroxide: from aquo to enzyme,
491 Coordination Chemistry Reviews, 233, 311-318, 2002.
492 Ervens, B., Feingold, G., Frost, G. J., and Kreidenweis, S. M.: A modeling study of aqueous
493 production of dicarboxylic acids: 1. Chemical pathways and speciated organic mass production,
494 Journal of Geophysical Research-Atmospheres, 109, D15205, 10.1029/2003jd004387, 2004.
495 Ervens, B., and Volkamer, R.: Glyoxal processing by aerosol multiphase chemistry: towards a
496 kinetic modeling framework of secondary organic aerosol formation in aqueous particles,
497 Atmospheric Chemistry and Physics, 10, 8219-8244, DOI 10.5194/acp-10-8219-2010, 2010.
498 Ervens, B., Turpin, B. J., and Weber, R. J.: Secondary organic aerosol formation in cloud droplets
499 and aqueous particles (aqSOA): a review of laboratory, field and model studies, Atmospheric

500 Chemistry and Physics, 11, 11069-11102, 10.5194/acp-11-11069-2011, 2011.
501 Ervens, B., Sorooshian, A., Lim, Y. B., and Turpin, B. J.: Key parameters controlling OH-initiated
502 formation of secondary organic aerosol in the aqueous phase (aqSOA), Journal of Geophysical
503 Research-Atmospheres, 119, 3997-4016, 10.1002/2013JD021021, 2014.
504 Ervens, B.: Modeling the Processing of Aerosol and Trace Gases in Clouds and Fogs, Chem Rev,
505 115, 4157-4198, 10.1021/cr5005887, 2015.
506 Fenton, H.: LXXIII.—Oxidation of tartaric acid in presence of iron, Journal of the Chemical
507 Society, Transactions, 65, 899-910, 1894.
508 Fountoukis, C., and Nenes, A.: ISORROPIA II: a computationally efficient thermodynamic
509 equilibrium model for K+–Ca 2+–Mg 2+–NH 4+–Na+–SO 4 2−–NO 3−–Cl−–H 2 O aerosols,
510 Atmospheric Chemistry and Physics, 7, 4639-4659, 2007.
511 Galloway, M. M., Chhabra, P. S., Chan, A. W. H., Surratt, J. D., Flagan, R. C., Seinfeld, J. H., and
512 Keutsch, F. N.: Glyoxal uptake on ammonium sulphate seed aerosol: reaction products and
513 reversibility of uptake under dark and irradiated conditions, Atmospheric Chemistry and
514 Physics, 9, 3331-3345, 10.5194/acp-9-3331-2009, 2009.
515 Gligorovski, S., Strekowski, R., Barbati, S., and Vione, D.: Environmental Implications of
516 Hydroxyl Radicals (•OH), Chem Rev, 115, 13051-13092, 10.1021/cr500310b, 2015.
517 Goldstein, A. H., and Galbally, I. E.: Known and unexplored organic constituents in the earth's
518 atmosphere, Environmental Science & Technology, 41, 1514-1521, Doi 10.1021/Es072476p,
519 2007.
520 Hallquist, M., Wenger, J. C., Baltensperger, U., Rudich, Y., Simpson, D., Claeys, M., Dommen, J.,
521 Donahue, N. M., George, C., Goldstein, A. H., Hamilton, J. F., Herrmann, H., Hoffmann, T.,
522 Iinuma, Y., Jang, M., Jenkin, M. E., Jimenez, J. L., Kiendler-Scharr, A., Maenhaut, W.,
523 McFiggans, G., Mentel, T. F., Monod, A., Prévôt, A. S. H., Seinfeld, J. H., Surratt, J. D.,
524 Szmigielski, R., and Wildt, J.: The formation, properties and impact of secondary organic
525 aerosol: current and emerging issues, Atmospheric Chemistry and Physics, 9, 5155-5236,
526 10.5194/acp-9-5155-2009, 2009.
527 Hanson, D. R., Burkholder, J. B., Howard, C. J., and Ravishankara, A.: Measurement of hydroxyl
528 and hydroperoxy radical uptake coefficients on water and sulfuric acid surfaces, The Journal of
529 Physical Chemistry, 96, 4979-4985, 1992.
530 Hatch, L. E., Creamean, J. M., Ault, A. P., Surratt, J. D., Chan, M. N., Seinfeld, J. H., Edgerton, E.
531 S., Su, Y., and Prather, K. A.: Measurements of isoprene-derived organosulfates in ambient
532 aerosols by aerosol time-of-flight mass spectrometry-Part 1: Single particle atmospheric
533 observations in Atlanta, Environmental science & technology, 45, 5105-5111, 2011.
534 Herrmann, H., Tilgner, A., Barzaghi, P., Majdik, Z., Gligorovski, S., Poulain, L., and Monod, A.:
535 Towards a more detailed description of tropospheric aqueous phase organic chemistry:
536 CAPRAM 3.0, Atmospheric Environment, 39, 4351-4363, 10.1016/j.atmosenv.2005.02.016,
537 2005.
538 Herrmann, H., Schaefer, T., Tilgner, A., Styler, S. A., Weller, C., Teich, M., and Otto, T.:
539 Tropospheric Aqueous-Phase Chemistry: Kinetics, Mechanisms, and Its Coupling to a Changing
540 Gas Phase, Chem Rev, 115, 4259-4334, 10.1021/cr500447k, 2015.
541 Ho, K. F., Cao, J. J., Lee, S. C., Kawamura, K., Zhang, R. J., Chow, J. C., and Watson, J. G.:
542 Dicarboxylic acids, ketocarboxylic acids, and dicarbonyls in the urban atmosphere of China,
543 Journal of Geophysical Research-Atmospheres, 112, D22S27, 10.1029/2006jd008011, 2007.

544 Ho, K. F., Lee, S. C., Ho, S. S. H., Kawamura, K., Tachibana, E., Cheng, Y., and Zhu, T.:
545 Dicarboxylic acids, ketocarboxylic acids, alpha-dicarbonyls, fatty acids, and benzoic acid in
546 urban aerosols collected during the 2006 Campaign of Air Quality Research in Beijing
547 (CAREBeijing-2006), Journal of Geophysical Research-Atmospheres, 115, D19312,
548 10.1029/2009jd013304, 2010.
549 Ho, K. F., Ho, S. S. H., Lee, S. C., Kawamura, K., Zou, S. C., Cao, J. J., and Xu, H. M.: Summer
550 and winter variations of dicarboxylic acids, fatty acids and benzoic acid in PM(2.5) in Pearl
551 Delta River Region, China, Atmospheric Chemistry and Physics, 11, 2197-2208,
552 10.5194/acp-11-2197-2011, 2011.
553 Huang, X.-F., and Yu, J. Z.: Is vehicle exhaust a significant primary source of oxalic acid in
554 ambient aerosols?, Geophysical Research Letters, 34, L02808, 10.1029/2006gl028457, 2007.
555 Jimenez, J. L., Canagaratna, M. R., Donahue, N. M., Prevot, A. S. H., Zhang, Q., Kroll, J. H.,
556 DeCarlo, P. F., Allan, J. D., Coe, H., Ng, N. L., Aiken, A. C., Docherty, K. S., Ulbrich, I. M.,
557 Grieshop, A. P., Robinson, A. L., Duplissy, J., Smith, J. D., Wilson, K. R., Lanz, V. A., Hueglin,
558 C., Sun, Y. L., Tian, J., Laaksonen, A., Raatikainen, T., Rautiainen, J., Vaattovaara, P., Ehn, M.,
559 Kulmala, M., Tomlinson, J. M., Collins, D. R., Cubison, M. J., Dunlea, E. J., Huffman, J. A.,
560 Onasch, T. B., Alfarra, M. R., Williams, P. I., Bower, K., Kondo, Y., Schneider, J., Drewnick, F.,
561 Borrmann, S., Weimer, S., Demerjian, K., Salcedo, D., Cottrell, L., Griffin, R., Takami, A.,
562 Miyoshi, T., Hatakeyama, S., Shimono, A., Sun, J. Y., Zhang, Y. M., Dzepina, K., Kimmel, J. R.,
563 Sueper, D., Jayne, J. T., Herndon, S. C., Trimborn, A. M., Williams, L. R., Wood, E. C.,
564 Middlebrook, A. M., Kolb, C. E., Baltensperger, U., and Worsnop, D. R.: Evolution of Organic
565 Aerosols in the Atmosphere, Science, 326, 1525-1529, 10.1126/science.1180353, 2009.
566 Kawamura, K., and Ikushima, K.: seasonal-changes in the distribution of dicarboxylic-acids in the
567 urban atmosphere, Environmental Science & Technology, 27, 2227-2235, 10.1021/es00047a033,
568 1993.
569 Kawamura, K., Kobayashi, M., Tsubonuma, N., Mochida, M., Watanabe, T., and Lee, M.: Organic
570 and inorganic compositions of marine aerosols from East Asia: Seasonal variations of
571 water-soluble dicarboxylic acids, major ions, total carbon and nitrogen, and stable C and N
572 isotopic composition, Geochemical Investigations in Earth and Space Science: A Tribute to
573 Issac R. Kaplan, 9, edited by: Hill, R. J. L. J. A. Z. B. M. J. C. G., and Eganhouse, R. G. M. P.
574 K., 243-265 pp., 2004.
575 Kawamura, K., and Yasui, O.: Diurnal changes in the distribution of dicarboxylic acids,
576 ketocarboxylic acids and dicarbonyls in the urban Tokyo atmosphere, Atmospheric
577 Environment, 39, 1945-1960, 10.1016/j.atmosenv.2004.12.014, 2005.
578 Kawamura, K., Kasukabe, H., and Barrie, L. A.: Secondary formation of water-soluble organic
579 acids and alpha-dicarbonyls and their contributions to total carbon and water-soluble organic
580 carbon: Photochemical aging of organic aerosols in the Arctic spring, Journal of Geophysical
581 Research-Atmospheres, 115, D21306, 10.1029/2010jd014299, 2010.
582 Kawamura, K., Tachibana, E., Okuzawa, K., Aggarwal, S. G., Kanaya, Y., and Wang, Z. F.: High
583 abundances of water-soluble dicarboxylic acids, ketocarboxylic acids and alpha-dicarbonyls in
584 the mountaintop aerosols over the North China Plain during wheat burning season, Atmospheric
585 Chemistry and Physics, 13, 8285-8302, 10.5194/acp-13-8285-2013, 2013.
586 Khezri, B., Mo, H., Yan, Z., Chong, S.-L., Heng, A. K., and Webster, R. D.: Simultaneous online
587 monitoring of inorganic compounds in aerosols and gases in an industrialized area, Atmospheric

588 Environment, 80, 352-360, 2013.
589 Kremer, M. L.: The Fenton reaction. Dependence of the rate on pH, Journal of Physical Chemistry
590 A, 107, 1734-1741, 10.1021/jp020654p, 2003.
591 Kundu, S., Kawamura, K., Andreae, T. W., Hoffer, A., and Andreae, M. O.: Molecular
592 distributions of dicarboxylic acids, ketocarboxylic acids and alpha-dicarbonyls in biomass
593 burning aerosols: implications for photochemical production and degradation in smoke layers,
594 Atmospheric Chemistry and Physics, 10, 2209-2225, 10.5194/acp-10-2209-2010, 2010.
595 Li, L., Huang, Z. X., Dong, J. G., Li, M., Gao, W., Nian, H. Q., Fu, Z., Zhang, G. H., Bi, X. H.,
596 Cheng, P., and Zhou, Z.: Real time bipolar time-of-flight mass spectrometer for analyzing single
597 aerosol particles, Int J Mass Spectrom, 303, 118-124, 10.1016/j.ijms.2011.01.017, 2011.
598 Li, L., Li, M., Huang, Z., Gao, W., Nian, H., Fu, Z., Gao, J., Chai, F., and Zhou, Z.: Ambient
599 particle characterization by single particle aerosol mass spectrometry in an urban area of Beijing,
600 Atmospheric Environment, 94, 323-331, 2014.
601 Lim, Y. B., Tan, Y., Perri, M. J., Seitzinger, S. P., and Turpin, B. J.: Aqueous chemistry and its role
602 in secondary organic aerosol (SOA) formation, Atmospheric Chemistry and Physics, 10,
603 10521-10539, 10.5194/acp-10-10521-2010, 2010.
604 Ma, Q. X., He, H., and Liu, C.: Hygroscopic properties of oxalic acid and atmospherically relevant
605 oxalates, Atmospheric Environment, 69, 281-288, 10.1016/j.atmosenv.2012.12.011, 2013.
606 Ma, S. X., Ren, K., Liu, X. W., Chen, L. G., Li, M., Li, X. Y., Yang, J., Huang, B., Zheng, M., and
607 Xu, Z. C.: Production of hydroxyl radicals from Fe-containing fine particles in Guangzhou,
608 China, Atmospheric Environment, 123, 72-78, 10.1016/j.atmosenv.2015.10.057, 2015.
609 McNeill, V. F.: Aqueous organic chemistry in the atmosphere: Sources and chemical processing of
610 organic aerosols, Environmental science & technology, 49, 1237-1244, 2015.
611 Meng, J., Wang, G., Li, J., Cheng, C., Ren, Y., Huang, Y., Cheng, Y., Cao, J., and Zhang, T.:
612 Seasonal characteristics of oxalic acid and related SOA in the free troposphere of Mt. Hua,
613 central China: Implications for sources and formation mechanisms, Science Of The Total
614 Environment, 493, 1088-1097, 10.1016/j.scitotenv.2014.04.086, 2014.
615 Meng, J. J., Wang, G. H., Li, J. J., Cheng, C. L., and Cao, J. J.: Atmospheric oxalic acid and
616 related secondary organic aerosols in Qinghai Lake, a continental background site in Tibet
617 Plateau, Atmospheric Environment, 79, 582-589, 10.1016/j.atmosenv.2013.07.024, 2013.
618 Miyazaki, Y., Aggarwal, S. G., Singh, K., Gupta, P. K., and Kawamura, K.: Dicarboxylic acids and
619 water-soluble organic carbon in aerosols in New Delhi, India, in winter: Characteristics and
620 formation processes, Journal of Geophysical Research-Atmospheres, 114, D19206,
621 10.1029/2009jd011790, 2009.
622 Moffet, R. C., de Foy, B., Molina, L. T., Molina, M. J., and Prather, K. A.: Measurement of
623 ambient aerosols in northern Mexico City by single particle mass spectrometry, Atmospheric
624 Chemistry and Physics, 8, 4499-4516, 10.5194/acp-8-4499-2008, 2008.
625 Myriokefalitakis, S., Tsigaridis, K., Mihalopoulos, N., Sciare, J., Nenes, A., Kawamura, K., Segers,
626 A., and Kanakidou, M.: In-cloud oxalate formation in the global troposphere: a 3-D modeling
627 study, Atmospheric Chemistry and Physics, 11, 5761-5782, 10.5194/acp-11-5761-2011, 2011.
628 Nenes, A., Pandis, S. N., and Pilinis, C.: ISORROPIA: A new thermodynamic equilibrium model
629 for multiphase multicomponent inorganic aerosols, Aquatic geochemistry, 4, 123-152, 1998.
630 Nenes, A., Pandis, S. N., and Pilinis, C.: Continued development and testing of a new
631 thermodynamic aerosol module for urban and regional air quality models, Atmospheric

Environment, 33, 1553-1560, 1999.

Noble, C. A., and Prather, K. A.: Real-time measurement of correlated size and composition profiles of individual atmospheric aerosol particles, Environmental science & technology, 30, 2667-2680, 1996.

Novakov, T., and Penner, J. E.: Large Contribution of Organic Aerosols to Cloud-Condensation-Nuclei Concentrations, Nature, 365, 823-826, Doi 10.1038/365823a0, 1993.

Pavuluri, C. M., Kawamura, K., and Swaminathan, T.: Water-soluble organic carbon, dicarboxylic acids, ketoacids, and alpha-dicarbonyls in the tropical Indian aerosols, Journal of Geophysical Research-Atmospheres, 115, D11302, 10.1029/2009JD012661, 2010.

Poschl, U., and Shiraiwa, M.: Multiphase Chemistry at the Atmosphere-Biosphere Interface Influencing Climate and Public Health in the Anthropocene, Chem Rev, 115, 4440-4475, 10.1021/cr500487s, 2015.

Prather, K. A., Nordmeyer, T., and Salt, K.: Real-time characterization of individual aerosol particles using time-of-flight mass spectrometry, Anal. Chem., 66, 1403-1407, 1994.

Prenni, A. J., De Mott, P. J., and Kreidenweis, S. M.: Water uptake of internally mixed particles containing ammonium sulfate and dicarboxylic acids, Atmospheric Environment, 37, 4243-4251, 10.1016/s1352-2310(03)00559-4, 2003.

Silva, P. J., and Prather, K. A.: Interpretation of mass spectra from organic compounds in aerosol time-of-flight mass spectrometry, Analytical Chemistry, 72, 3553-3562, 2000.

Sorooshian, A., Lu, M.-L., Brechtel, F. J., Jonsson, H., Feingold, G., Flagan, R. C., and Seinfeld, J. H.: On the source of organic acid aerosol layers above clouds, Environmental Science & Technology, 41, 4647-4654, 10.1021/es0630442, 2007.

Sorooshian, A., Wang, Z., Coggon, M. M., Jonsson, H. H., and Ervens, B.: Observations of Sharp Oxalate Reductions in Stratocumulus Clouds at Variable Altitudes: Organic Acid and Metal Measurements During the 2011 E-PEACE Campaign, Environmental Science & Technology, 47, 7747-7756, 10.1021/es4012383, 2013.

Stone, E. A., Hedman, C. J., Zhou, J. B., Mieritz, M., and Schauer, J. J.: Insights into the nature of secondary organic aerosol in Mexico City during the MILAGRO experiment 2006, Atmospheric Environment, 44, 312-319, 10.1016/j.atmosenv.2009.10.036, 2010.

Sullivan, R. C., and Prather, K. A.: Investigations of the diurnal cycle and mixing state of oxalic acid in individual particles in Asian aerosol outflow, Environmental Science & Technology, 41, 8062-8069, 10.1021/es071134g, 2007.

Surratt, J. D., Kroll, J. H., Kleindienst, T. E., Edney, E. O., Claeys, M., Sorooshian, A., Ng, N. L., Offenberg, J. H., Lewandowski, M., Jaoui, M., Flagan, R. C., and Seinfeld, J. H.: Evidence for organosulfates in secondary organic aerosol, Environmental Science & Technology, 41, 517-527, 10.1021/Es062081q, 2007.

Surratt, J. D., Gomez-Gonzalez, Y., Chan, A. W. H., Vermeylen, R., Shahgholi, M., Kleindienst, T. E., Edney, E. O., Offenberg, J. H., Lewandowski, M., Jaoui, M., Maenhaut, W., Claeys, M., Flagan, R. C., and Seinfeld, J. H.: Organosulfate formation in biogenic secondary organic aerosol, Journal of Physical Chemistry A, 112, 8345-8378, Doi 10.1021/Jp802310p, 2008.

ten Brink, H., Otjes, R., Jongejan, P., and Slanina, S.: An instrument for semi-continuous monitoring of the size-distribution of nitrate, ammonium, sulphate and chloride in aerosol, Atmospheric Environment, 41, 2768-2779, 2007.

676 Tong, H. J., Arangio, A. M., Lakey, P. S. J., Berkemeier, T., Liu, F. B., Kampf, C. J., Brune, W. H.,
677 Poschl, U., and Shiraiwa, M.: Hydroxyl radicals from secondary organic aerosol decomposition
678 in water, Atmospheric Chemistry and Physics, 16, 1761-1771, 10.5194/acp-16-1761-2016,
679 2016.
680 van Pinxteren, D., Neususs, C., and Herrmann, H.: On the abundance and source contributions of
681 dicarboxylic acids in size-resolved aerosol particles at continental sites in central Europe,
682 Atmospheric Chemistry and Physics, 14, 3913-3928, 10.5194/acp-14-3913-2014, 2014.
683 Wang, G., Kawamura, K., Cheng, C., Li, J., Cao, J., Zhang, R., Zhang, T., Liu, S., and Zhao, Z.:
684 Molecular Distribution and Stable Carbon Isotopic Composition of Dicarboxylic Acids,
685 Ketocarboxylic Acids, and alpha-Dicarbonyls in Size-Resolved Atmospheric Particles From
686 Xi'an City, China, Environmental Science & Technology, 46, 4783-4791, 10.1021/es204322c,
687 2012.
688 Weller, C., Tilgner, A., Brauer, P., and Herrmann, H.: Modeling the Impact of Iron-Carboxylate
689 Photochemistry on Radical Budget and Carboxylate Degradation in Cloud Droplets and
690 Particles, Environmental Science & Technology, 48, 5652-5659, 10.1021/es4056643, 2014.
691 Xue, J., Lau, A. K. H., and Yu, J. Z.: A study of acidity on PM2.5 in Hong Kong using online ionic
692 chemical composition measurements, Atmospheric Environment, 45, 7081-7088,
693 10.1016/j.atmosenv.2011.09.040, 2011.
694 Yang, F., Chen, H., Wang, X., Yang, X., Du, J., and Chen, J.: Single particle mass spectrometry of
695 oxalic acid in ambient aerosols in Shanghai: Mixing state and formation mechanism,
696 Atmospheric Environment, 43, 3876-3882, 2009.
697 Yao, X. H., Fang, M., and Chan, C. K.: Size distributions and formation of dicarboxylic acids in
698 atmospheric particles, Atmospheric Environment, 36, 2099-2107, 2002.
699 Yao, X. H., Lau, A. P. S., Fang, M., Chan, C. K., and Hu, M.: Size distributions and formation of
700 ionic species in atmospheric particulate pollutants in Beijing, China: 2 - dicarboxylic acids,
701 Atmospheric Environment, 37, 3001-3007, 10.1016/s1352-2310(03)00256-5, 2003.
702 Yu, J. Z., Huang, X. F., Xu, J. H., and Hu, M.: When aerosol sulfate goes up, so does oxalate:
703 Implication for the formation mechanisms of oxalate, Environmental Science & Technology, 39,
704 128-133, 10.1021/Es049559f, 2005.
705 Yu, L., Smith, J., Laskin, A., Anastasio, C., Laskin, J., and Zhang, Q.: Chemical characterization
706 of SOA formed from aqueous-phase reactions of phenols with the triplet excited state of
707 carbonyl and hydroxyl radical, Atmospheric Chemistry and Physics, 14, 13801-13816,
708 10.5194/acp-14-13801-2014, 2014.
709 Zauscher, M. D., Wang, Y., Moore, M. J. K., Gaston, C. J., and Prather, K. A.: Air Quality Impact
710 and Physicochemical Aging of Biomass Burning Aerosols during the 2007 San Diego Wildfires,
711 Environmental Science & Technology, 47, 7633-7643, 10.1021/es4004137, 2013.
712 Zhang, G., Bi, X., Li, L., Chan, L. Y., Li, M., Wang, X., Sheng, G., Fu, J., and Zhou, Z.: Mixing
713 state of individual submicron carbon-containing particles during spring and fall seasons in
714 urban Guangzhou, China: a case study, Atmospheric Chemistry and Physics, 13, 4723-4735,
715 2013.
716 Zhang, G., Bi, X., He, J., Chen, D., Chan, L. Y., Xie, G., Wang, X., Sheng, G., Fu, J., and Zhou, Z.:
717 Variation of secondary coatings associated with elemental carbon by single particle analysis,
718 Atmospheric Environment, 92, 162-170, 2014.
719 Zhang, R., Wang, G., Guo, S., Zamora, M. L., Ying, Q., Lin, Y., Wang, W., Hu, M., and Wang, Y.:

Atmos. Chem. Phys. Discuss., doi:10.5194/acp-2016-1081, 2016
Manuscript under review for journal Atmos. Chem. Phys.
Published: 21 December 2016

720 Formation of urban fine particulate matter, Chem Rev, 115, 3803-3855, 2015.
721 Zhou, Y., Huang, X. H., Bian, Q., Griffith, S. M., Louie, P. K., and Yu, J. Z.: Sources and
722 atmospheric processes impacting oxalate at a suburban coastal site in Hong Kong: Insights
723 inferred from 1 year hourly measurements, Journal of Geophysical Research: Atmospheres, 120,
724 9772-9788, 2015.
725
726
727
728
729
730
731
732
733
734
735
736
737
738
739
740
741
742
743
744
745
746
747
748
749
750
751
752
753
754
755
756
757
758
759
760
761
762
763

Atmos. Chem. Phys. Discuss., doi:10.5194/acp-2016-1081, 2016
Manuscript under review for journal Atmos. Chem. Phys.
Published: 21 December 2016

Atmospheric Chemistry and Physics Discussions

Tables and Figures

Table list:

Table 1. Summary of major groups of oxalic acid-containing particles in summer and winter in PRD, China.

Table 2. The abundance of major particle types in total oxalic acid-containing particles during the episode in winter (2/8/2015).

Figure caption:

Figure 1. Temporal variations of total detected particles and oxalic acid containing particles during whole sampling periods in Heshan, China: (a) hourly variations of $PM_{2.5}$ mass concentration, total detected particle counts, oxalic acid containing particles, ratio of oxalic acid-containing/total particles and major types of oxalic acid containing particles; (b) variation patterns of relative abundance of major types of oxalic acid containing particles.

Figure 2. The averaged positive and negative ion mass spectra of oxalic acid containing particles is investigated in summer and winter: (a) summer positive, (b) summer negative, (c) winter positive, (d) winter negative. The color bars represent each peak area corresponding to specific fraction in individual particles.

Figure 3. (a) Mixing state of oxalic acid with sulfate, nitrate and ammonium in oxalic acid-containing particles; (b) Linear correlation between NH_4^+-containing oxalic acid particles and the total oxalic acid particles in summer; (c) Linear correlation between NH_4^+-containing oxalic acid particles and the total oxalic acid particles in winter. Abbreviations: C_2-NH_4^+ represents the NH_4^+-containing oxalic acid particles, and same expressions for C_2-SO_4^{2-} and C_2-NO_3^-.

Atmos. Chem. Phys. Discuss., doi:10.5194/acp-2016-1081, 2016
Manuscript under review for journal Atmos. Chem. Phys.
Published: 21 December 2016

795 Figure 4. Unscaled size-resolved number distributions of major types of oxalic acid
796 particles in summer and winter.
797
798 Figure 5. Temporal variations of O_3 concentrations, oxalic acid particles, malonic acid
799 particles and heavy metal type of oxalic acid particles during the entire sampling
800 period in Heshan, China.
801
802 Figure 6. The averaged digitized positive and negative ion mass spectra of heavy
803 metal type of oxalic acid-containing particles in summer.
804
805 Figure 7. The diurnal variations of O_3 concentration, oxalic acid particles, HM group
806 particles and in-situ pH (pH_{is}) from July 28 to August 1 in 2014.
807
808 Figure 8. The formation process of oxalic acid in the aqueous phase of particles in
809 summer: the red steps are enhanced by photochemical activities in the current study.
810
811 Figure 9. The comprehensive study of oxalic acid particles increase on Feb 8, 2015: (a)
812 The digitized positive and negative ion mass spectrum of oxalic acid particles during
813 the episode; (b) Linear regression between oxalic acid particles and organosulfate
814 particles (m/z -155).
815
816
817
818
819
820
821
822
823
824

Atmos. Chem. Phys. Discuss., doi:10.5194/acp-2016-1081, 2016
Manuscript under review for journal Atmos. Chem. Phys.
Published: 21 December 2016

Atmospheric Chemistry and Physics Discussions

825

826

827

Table 1. Summary of major groups of oxalic acid-containing particles in summer and winter in PRD, China.

	Summer(7/18-8/1, 2014)		Winter(1/27-2/8, 2015)	
Particle type	Count	Percentage, %	Count	Percentage, %
EC	1473	11.2	3161	15.4
ECOC	41	0.3	2233	10.9
OC	473	3.6	1922	9.4
BB	1702	13.0	4953	24.2
HM	4104	31.3	3124	15.2
Sec	2511	19.2	2192	10.7
NaK	303	2.3	17	0.1
Dust	1139	8.7	1888	9.2

Abbreviations of major particle types: elemental carbon (EC), elemental and organic carbon (ECOC), organic carbon (OC), biomass burning (BB), heavy metal (HM), secondary (Sec), sodium and potassium (NaK) and dust (Dust).

828

829

830

831

832

Table 2. The abundance of major particle types in total oxalic acid-containing particles during the episode in winter (2/8/2015).

	EC	ECOC	OC	BB	Sec	HM	Dust	other
Count	1250	604	326	1320	856	377	814	132
Percentage, %	22.0	10.6	5.7	23.2	15.1	6.6	14.3	2.3

833

834

835

836

837

838

839

840

841

842

843

844

845

846

847

Atmos. Chem. Phys. Discuss., doi:10.5194/acp-2016-1081, 2016
Manuscript under review for journal Atmos. Chem. Phys.
Published: 21 December 2016

Atmospheric Chemistry and Physics Discussions

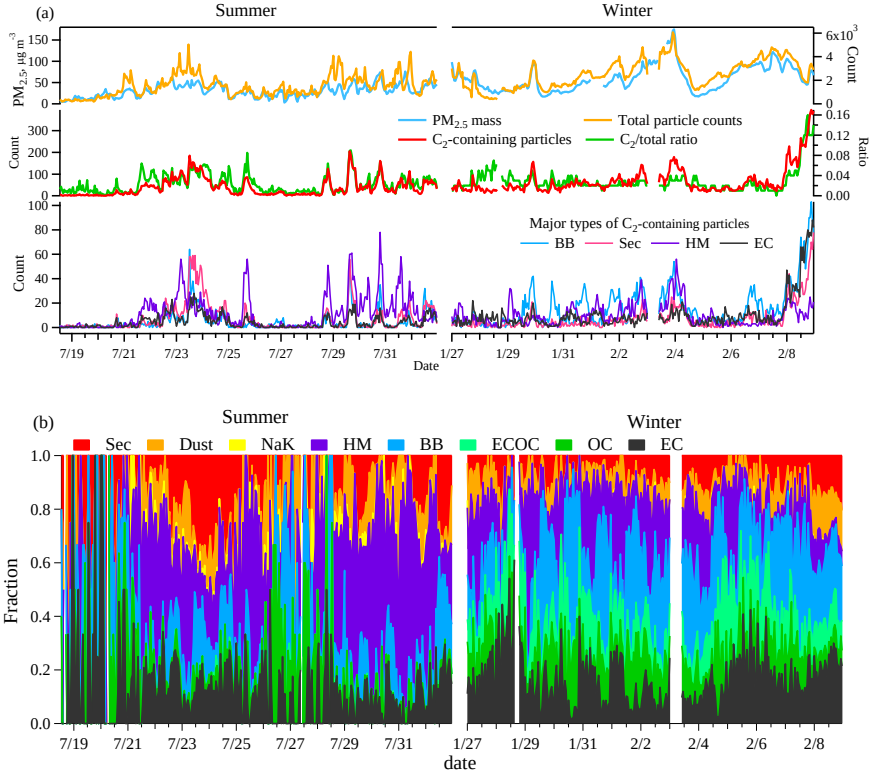

Figure 1. Temporal variations of total detected particles and oxalic acid containing particles during whole sampling periods in Heshan, China: (a) hourly variations of $PM_{2.5}$ mass concentration, total detected particle counts, oxalic acid containing particles, ratio of oxalic acid-containing/total particles and major types of oxalic acid containing particles; (b) variation patterns of relative abundance of major types of oxalic acid containing particles. Abbreviations of major particle types: elemental carbon (EC), organic carbon (OC), elemental and organic carbon (ECOC), biomass burning (BB), heavy metal (HM), secondary (Sec), sodium and potassium (NaK) and dust.

Atmos. Chem. Phys. Discuss., doi:10.5194/acp-2016-1081, 2016
Manuscript under review for journal Atmos. Chem. Phys.
Published: 21 December 2016

Atmospheric Chemistry and Physics Discussions

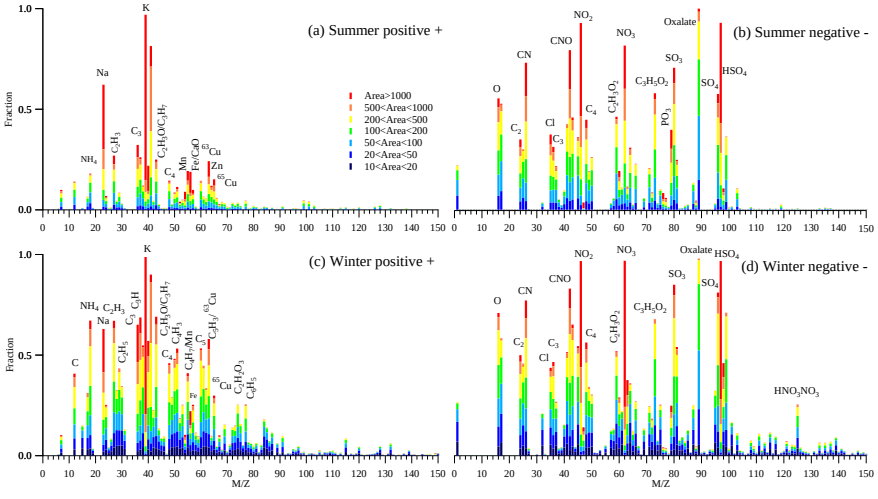

Figure 2. The averaged positive and negative ion mass spectra of oxalic acid containing particles is investigated in summer and winter: (a) summer positive, (b) summer negative, (c) winter positive, (d) winter negative. The color bars represent each peak area corresponding to specific fraction in individual particles.

Atmos. Chem. Phys. Discuss., doi:10.5194/acp-2016-1081, 2016
Manuscript under review for journal Atmos. Chem. Phys.
Published: 21 December 2016

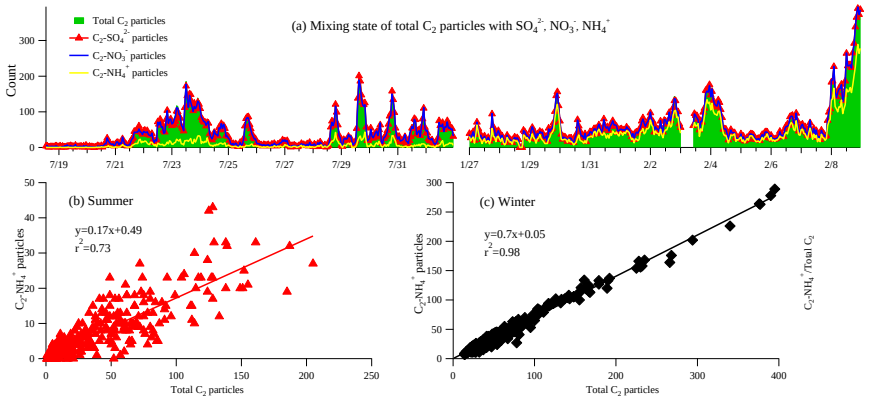

Figure 3. (a) Mixing state of oxalic acid with sulfate, nitrate and ammonium in oxalic acid-containing particles; (b) Linear correlation between NH_4^+-containing oxalic acid particles and the total oxalic acid particles in summer; (c) Linear correlation between NH_4^+-containing oxalic acid particles and the total oxalic acid particles in winter. Abbreviations: C_2-NH_4^+ represents the NH_4^+-containing oxalic acid particles, and same expressions for C_2-SO_4^{2-} and C_2-NO_3^-.

Atmos. Chem. Phys. Discuss., doi:10.5194/acp-2016-1081, 2016
Manuscript under review for journal Atmos. Chem. Phys.
Published: 21 December 2016

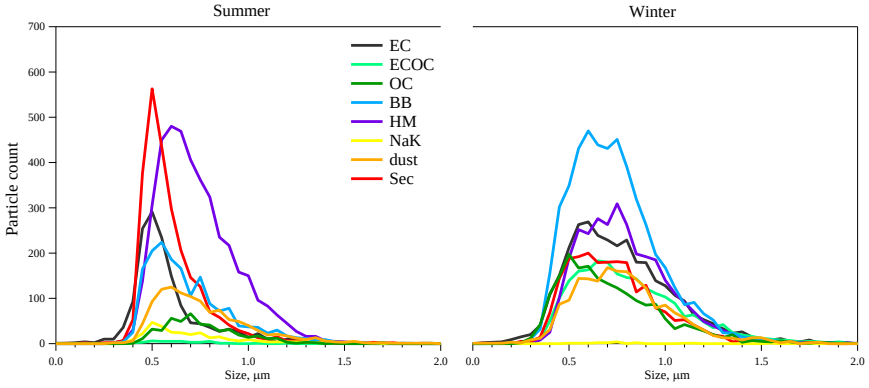

Figure 4. Unscaled size-resolved number distributions of major types of oxalic acid particles in summer and winter. Abbreviations of major particle types: elemental carbon (EC), organic carbon (OC), elemental and organic carbon (ECOC), biomass burning (BB), heavy metal (HM), secondary (Sec), sodium and potassium (NaK) and dust.

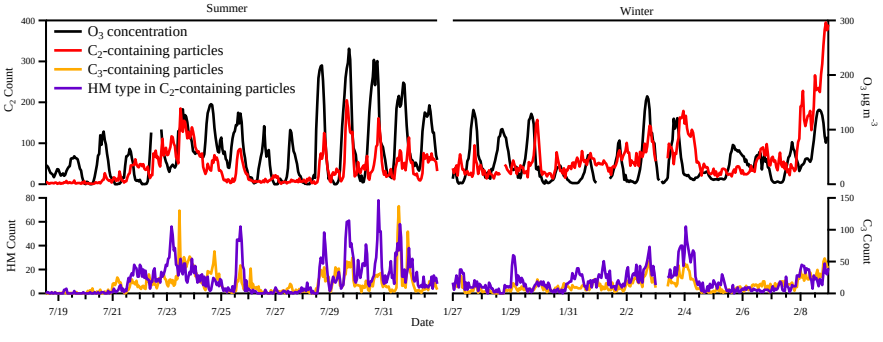

Figure 5. Temporal variations of O_3 concentrations, oxalic acid particles, malonic acid particles and heavy metal type of oxalic acid particles during the entire sampling period in Heshan, China.

Atmos. Chem. Phys. Discuss., doi:10.5194/acp-2016-1081, 2016
Manuscript under review for journal Atmos. Chem. Phys.
Published: 21 December 2016

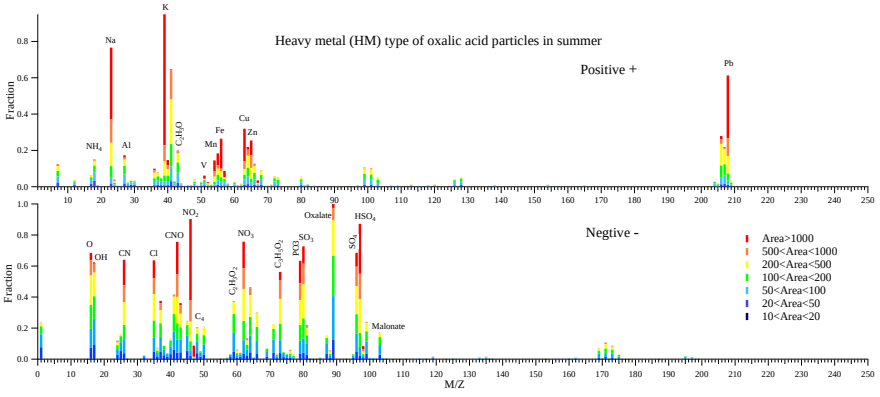

931

932 Figure 6. The averaged digitized positive and negative ion mass spectra of heavy
933 metal type of oxalic acid-containing particles in summer.

934

935

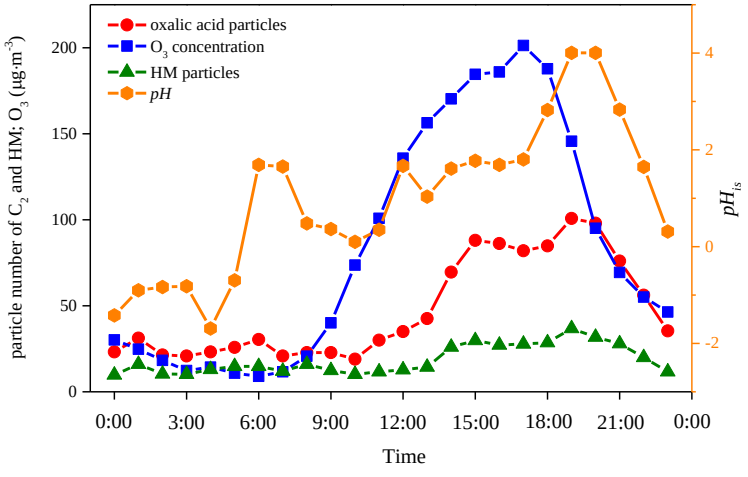

936

937 Figure 7. The diurnal variations of O_3 concentration, oxalic acid particles, HM group
938 particles and in-situ pH (pH_{is}) from July 28 to August 1 in 2014.

939

940

941

942

943

944

Atmos. Chem. Phys. Discuss., doi:10.5194/acp-2016-1081, 2016
Manuscript under review for journal Atmos. Chem. Phys.
Published: 21 December 2016

Atmospheric Chemistry and Physics Discussions

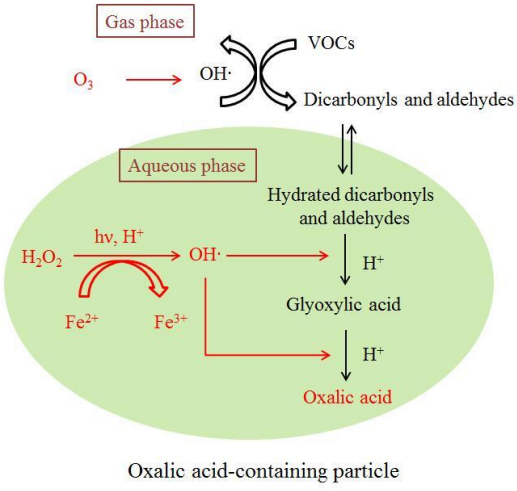

Figure 8. The formation process of oxalic acid in the aqueous phase of particles in summer: the red steps are enhanced by photochemical activities in the current study.

Atmos. Chem. Phys. Discuss., doi:10.5194/acp-2016-1081, 2016
Manuscript under review for journal Atmos. Chem. Phys.
Published: 21 December 2016

Atmospheric Chemistry and Physics Discussions

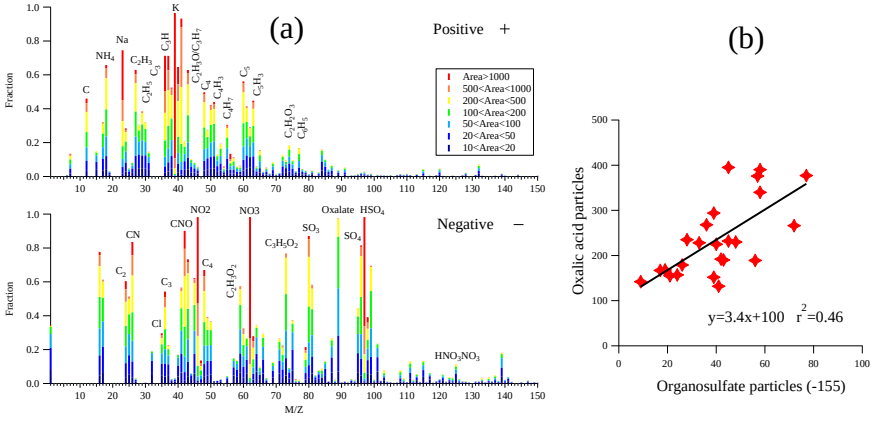

Figure 9. The comprehensive study of oxalic acid particles increase on Feb 8, 2015: (a) The digitized positive and negative ion mass spectrum of oxalic acid particles during the episode; (b) Linear regression between oxalic acid particles and organosulfate particles (m/z -155).